Symmetry-Adapted Perturbation Theory Analysis of the N···HX Hydrogen Bonds

Jarosław J. Panek* and Aneta Jezierska

University of Wrocław, Faculty of Chemistry, ul. F. Joliot-Curie 14, 50-383 Wrocław, Poland

Received: May 25, 2006; In Final Form: October 6, 2006

The main aim of the study was the detailed investigation of the interaction energy decomposition in dimers and trimers containing N···HX bonds of different types. The study of angular dependence of interaction energy terms partitioned according to the symmetry-adapted perturbation theory (SAPT) was performed for the dimers containing N···HX bonds as mentioned above: ammonia−HX (X = F, Cl, Br) and pyridine−HF complexes. It was found that the electrostatic and induction terms exhibit strong angular dependence, while the exchange contributions are less affected. The dispersion terms are virtually nondirectional. In addition, the three-body SAPT interaction energy analysis for the mixed acid−base NH_3···$(HF)_2$ and $(NH_3)_2$···HF trimers revealed strong differences between interactions of similar strength but different types (i.e., hydrogen bond and general electrostatic interaction). The importance of the induction terms for the nonadditivity of the interaction energy in strongly polar systems was confirmed.

1. Introduction

The hydrogen bond is one of the most vigorously investigated types of interactions. It plays a crucial role in many areas of chemistry, especially biochemistry. The nature of the hydrogen bond is strictly dependent on the system, however, the scope of the term "hydrogen bond" is still evolving. Recent examples of its diversity are dihydrogen bonds ($D-H^{+}\cdots{}^{-}H-M$) and inverse ($Li^{+-}H^{-}\cdots Li^{+}$) hydrogen bonds.[1] The weak C−H···O interactions are recognized nowadays to be significant factors for protein structure features.[2,3] On the other hand, very short and strong symmetrical hydrogen bridges are found among small ionic complexes[4] and are thought responsible for some enzymatic reactions.[5−12] Inorganic compounds containing transition metals are sources of new nonclassical hydrogen bonds.[13] Even among noble gas complexes, there are some indications of hydrogen-bond-like behavior.[14] "Blue shift" phenomena have been widely investigated[15−20] for the last several years as probably the most controversial extension of the hydrogen bond family. Their nature is still debated, because various models are presented. These models try to explain the blue shift phenomena either in close relation or in opposition to the classical hydrogen bond.[15−20] The formal definition of the hydrogen bond would almost certainly mention its directionality, which makes the hydrogen bond one of the most important structure-building factors in, for example, molecular crystals and biological systems. This directionality is, undoubtedly, very important in distinguishing between hydrogen bonds and van der Waals forces. The study presented below is therefore performed for simple, well-defined complexes with strong hydrogen bonds and a limited number of additional interactions. Such benchmarking based on small molecules is well-known in interaction energy analysis studies.[21,22] The selected complexes comprise various choices of donor atoms (H_3N···HX with X = F, Cl, Br). These three systems have been thoroughly studied experimentally via IR and microwave spectroscopy,[23−27] and despite their simplicity, advanced calculations are necessary to predict details of the acidic proton position[28] or vibrational spectra.[29] Additionally, variation of the acceptor atom environment was studied by including a system with delocalized π electrons−pyridine···HF complex as a counterpart to the H_3N···HF. Inclusion of the two trimeric structures has been dictated by our desire to study the influence of a perturbation (a loosely linked third molecule) on the energy partitioning of a two-body interaction. Our contribution is aimed at the theoretical investigations on the basis of advanced interaction energy partitioning schemes to shed light on the extent and physical basis of hydrogen bond directionality and importance of three-body contributions in hydrogen-bonded systems. This, in turn, will give indication of the hydrogen bond behavior for more extended systems. The outline of the article is as follows: section 2 contains the details of the computational procedures applied during the study. Section 3 is devoted, in turn, to discussion of the interaction energy for dimers and three-body contributions for trimers. Concluding remarks are given in the last section.

2. Computational Methodology

The NH_3···HX (X = F, Cl, Br) dimers reported in this manuscript were studied at MP2/aug-cc-pVTZ level, while for the trimers (NH_3···HF···HF and NH_3···HF···NH_3) the aug-cc-pVDZ basis set was applied.[30,31] The C_5H_5N···HF dimer was investigated on the basis of the mixed basis set: aug-cc-pVTZ on the hydrogen bridge atoms (N, H, F) and aug-cc-pVDZ for the carbon and hydrogen atoms of the aromatic ring. The MP2 calculations were performed using the frozen core approximation, with only valence electrons being correlated. The procedure was applied consistently from more time-consuming NH_3−HBr and pyridine−HF systems to the smaller complexes. In addition, reference calculations at various levels up to MP4(SDTQ)/aug-cc-pVTZ were performed for the trimers to be compared with the perturbative interaction energy analysis. Basis set superposition error (BSSE) corrected geometry optimization was performed with Gaussian03 package.[32] The BSSE affects the potential energy surface of a complex[33] leading to distorted structures, which in turn—as our test calculations have shown—

* To whom correspondence should be addressed. Tel.: +48 71 3757246, fax: +48 71 3282348, e-mail: jarek@elrond.chem.uni.wroc.pl.

10.1021/jp063217+ CCC: $37.00
Published on Web 01/06/2007

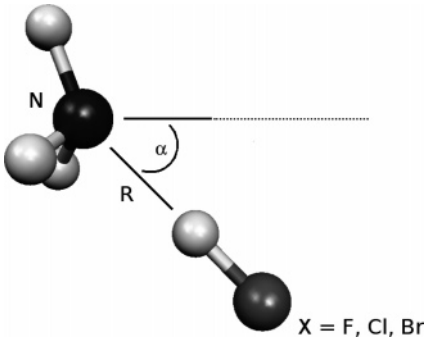

Figure 1. The structure of the investigated complexes with the distortion angle indicated. Positive values of α: the HX moves on the symmetry plane between the ammonia hydrogen atoms (or out of the pyridine ring plane).

yields artificially increased exchange contributions to the interaction energy of the studied systems. After the location of the equilibrium structures, symmetry-adapted perturbation theory (SAPT)[34] was employed for the interaction energy decomposition into contributions of well-defined physical meaning, for example, electrostatic, exchange, induction, and dispersion terms. The SAPT partitioning was performed with the same basis sets as used during the optimization, and the computational requirements of the SAPT scheme were limiting factors in the basis set choice. The calculated two-body SAPT energy included the unabridged set of the energy terms (labeled SAPT by the authors of the method, as opposed to the limited SAPT0 and SAPT2 schemes)[35] and consists of the following components:

$$E^{\mathrm{SAPT}} = E_{\mathrm{elst}}{}^{10} + E_{\mathrm{exch}}{}^{10} + E_{\mathrm{ind,r}}{}^{20} + E_{\mathrm{exch-ind,r}}{}^{20} + \delta\mathrm{HF}_{\mathrm{int,r}} + E_{\mathrm{elst,r}}{}^{12} + E_{\mathrm{elst,r}}{}^{13} + E_{\mathrm{disp}}{}^{20} + E_{\mathrm{exch-disp}}{}^{20} + {}^{\mathrm{t}}E_{\mathrm{ind}}{}^{22} + {}^{\mathrm{t}}E_{\mathrm{exch-ind}}{}^{22} + \epsilon_{\mathrm{exch}}{}^{1}(\mathrm{CCSD}) + \epsilon_{\mathrm{disp}}{}^{2} \quad (1)$$

Some of the components are calculated with coupled Hartree−Fock response of the perturbed system taken into account, which is denoted in the subscript, for example, $\delta\mathrm{HF}_{\mathrm{int,r}}$. The $\delta\mathrm{HF}_{\mathrm{int,r}}$ term, gathering higher order corrections to the uncorrelated interaction energy, was included in the calcuclations, as suggested by the SAPT implementation authors.[35] The intramonomer excitations up to the CCSD level are used in the calculations. The first four terms of the formula above yield the SCF SAPT energy (obtained without intramolecular electron correlation), and the remaining ones (without $\delta\mathrm{HF}_{\mathrm{int,r}}$) constitute the correlated part, $\mathrm{SAPT}_{\mathrm{corr,r}}$. The detailed description of the SAPT energy decomposition has been given in the defining papers.[34,35] The special version of the SAPT2002 package[35] with the three-body extensions coupled with GAMESS code[36] was used for the energy decomposition. The nonstandard three-body SAPT calculations, incorporating selected corrections to the exchange, exchange-induction, induction, and dispersion terms (see trimer SAPT columns of Tables 2 and 3), were performed on the basis of the methodology developed by Szalewicz et al.[37] The visualizations presented in the paper were prepared with the Molekel program.[38]

The angular dependence of various SAPT terms in the NH_3–HX dimers was performed in the following manner (see Figure 1): the HX molecule was kept at a constant distance, the same as in the equilibrium structure, from the basic moiety (ammonia or pyridine) with the angle between the HX and the base symmetry axis varying between 0 and 60 degrees in varying steps (every 3° up to 30°, then every 5° to 45°, and the final step was 60°). The movement was restricted to the symmetry plane of the base. Throughout the study, the following convention was assumed: positive values of the distortion angle indicate the movement of the HX molecule toward the bisection of the H−N−H angle in the ammonia or in the out-of-the-ring symmetry plane of the pyridine moiety. The negative angle values indicate that the HX molecule is moved toward the hydrogen atom of the ammonia or in the pyridine ring plane.

TABLE 1: Calculated Structural Parameters (in Å) of the Investigated Linear Hydrogen Bonds[d]

dimer	H−X	H···N	X···N	exp. X···N
NH_3···HF	0.9572	1.6390	2.5961	2.697[a]
NH_3···HCl	1.3276	1.6588	2.9864	3.137[b]
NH_3···HBr	1.4755	1.5275	3.0030	3.255[c]
pyridine···HF	0.9639	1.5820	2.5459	

[a] Reference 27. [b] References 24, 26. [c] Reference 25. [d] Available experimental data are listed for the X···N distance.

3. Results and Discussion

3.1. The NH_3···HX and C_5H_5N···HF Dimers. The optimized structures of the investigated NH_3···HX (X = F, Cl, Br) and C_5H_5N···HF dimers have linear N···HX hydrogen bonds with parameters given in Table 1. The N···H distance does not change monotonically, but when one takes into account also the growing H−X distance, it is seen that the degree of proton sharing is increasing in the HF, HCl, and HBr series. Therefore, it is expected that the perturbational method, such as SAPT scheme, will perform best for the HF complexes, where the separation of the system into the two noncovalently bonded subunits is most justified.

In general, the total SAPT interaction energy of the complexes is about −10 to −15 kcal/mol, with the ammonia−HF and pyridine−HF structures the strongest (−13.68 and −14.97 kcal/mol), ammonia−HCl in the middle (−9.70 kcal/mol), and ammonia−HBr the weakest (−9.45 kcal/mol). A previous study of the interaction energy partitioning in a diverse set of hydrogen-bonded systems[39] reports the interaction energy of −11.83 kcal/mol for the NH_3−HF complex at the MP2/6-311++G(d,p) structure. However, this result was obtained with the perturbative approach using MP2 method as the basis for the estimation of the correlated terms. The reported E_{CORR} is −0.40 kcal/mol.[39] The SAPT scheme used in the current work is believed to be of performance similar to the fourth-order Møller−Plesset method,[34,35] and the correlated terms might be held responsible for the deeper interaction well. Indeed, the $\mathrm{SAPT}_{\mathrm{corr,r}}$ values are −2.48, −4.87, −7.54, and −3.55 kcal/mol for the NH_3−HF, NH_3−HCl, NH_3−HBr, and pyridine−HF, respectively. At least for the NH_3−HF system, the additional 2 kcal/mol of the correlation energy is almost the exact difference between our result of −13.68 kcal/mol and the value of ref 39, thus supporting the validity of the energy partitioning schemes used in both cases. An additional observation is that the close proximity of an aromaticity basin leads to an almost 50% increase of the $\mathrm{SAPT}_{\mathrm{corr,r}}$ when comparing ammonia−HF and pyridine−HF, but this is a very small change with respect to the halogen substitution effects in the acid.

The interaction energy values alone would classify the systems studied as exhibiting strong hydrogen bonds (very strong intramolecular hydrogen bonds in FHF^- and maleate anions have energies of over 30 kcal/mol, in the range of the weakest covalent bonds). The alternative method of assessing the bond strength, a topological analysis of the electron localization function (ELF),[40] describes molecular space in terms of domains related to electron pairing, allowing one to study

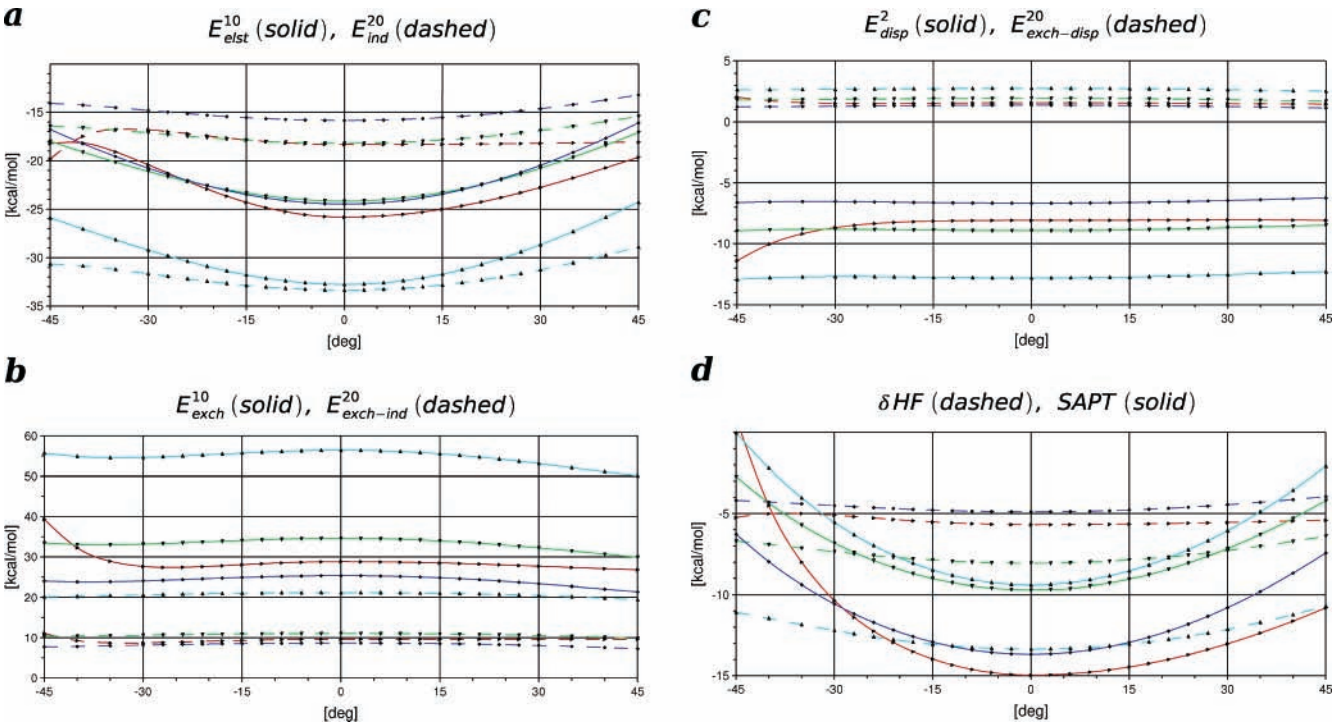

Figure 2. (a−d). Diagrams of the contributions to the interaction energy according to the SAPT scheme. Color coding for the diagrams: NH_3−HF, blue; NH_3−HCl, green; NH_3−HBr, light blue; pyridine−HF, red.

covalency and delocalization phenomena.[41] Using the ELF analysis, Fuster and Silvi assigned the studied ammonia−HX dimers to the middle strength type, with the category of "strong" hydrogen bonds reserved only for the dominantly covalent systems.[42] This fact, however, indicates that special care must be taken with regard to the reliability of the SAPT scheme, designed with weak interactions in mind. The growing degree of proton sharing, mentioned above, makes separation of the system into two distinct subunits problematic even for the NH_3−HCl complex and is the worst for the NH_3−HBr. The latter has acceptor−proton distance only 0.05 Å longer than the H−Br bond in the isolated HBr molecule, and thus this complex has a significant contribution of the $NH_4^+Br^-$ structure (but only in the presence of additional water molecules does the proton transfer become complete).[28] The δHF term (see Figure 2d), gathering the higher-order noncorrelated terms of the interaction energy, is a good indicator of this fact. It is rather small in comparison with the total interaction energy only for the HF complexes. Further, it is large for the NH_3−HCl complex and in case of NH_3−HBr even dominates the interaction energy. The intermolecular distances are similar in all the systems studied. Therefore, the large δHF values obtained for the HCl and HBr complexes are not results of the perturbation theory collapse because of small distance but of the covalency of the hydrogen bond. Further support for this statement will be found in the discussion of the trimers.

The results of the SAPT interaction energy partitioning for different distortion angle values are presented in Figure 2a−d. The diagrams show clearly that various contributions have a different angular dependence, which will be discussed below. The asymmetry of the diagrams is caused by differing definitions of the positive and negative distortion angles, see Figure 1. A detailed list of the energy partitioning results is available as the Supporting Information.

The electrostatic term E_{elst}^{10} is much more dependent on the angle than the induction term E_{ind}^{20} (Figure 2a). The former describes interaction between the permanent electric multipoles of the molecules and is therefore subject, in a crude approximation, to the behavior of dipole−dipole interactions. Both terms are highest for the NH_3−HBr complex involving the most polarizable acid. The polarizability variations in the studied halide series would explain the fact of the E_{ind}^{20} term being maximal for the HBr-containing system, but on the other hand, the E_{elst}^{10} term is related to the uncorrelated permanent electric multipole moments of the monomers. The experimental dipole moment values are in fact decreasing in the HF−HCl−HBr series (1.820D, 1.080D, and 0.827D, respectively),[43] and the explanation of the E_{elst}^{10} term ordering must clearly involve multipoles of a higher order. Indeed, comparison of the diagonal components of the quadrupole moment tensor for the HF and HCl (*xx*/*yy*/*zz* values are, respectively, −1.17/−1.17/2.34 and −1.92/−1.92/3.84 D·Å)[43] shows that the sequence is reversed and consistent with the calculated E_{elst}^{10} term trend.

Both exchange and exchange-induction terms are much less angular-dependent than the electrostatic and induction terms (Figure 2b). This is directly related to the fact that the investigated hydrogen bonds are not predominantly covalent. The covalent character is strongest at the linear arrangement of atoms, therefore, the E_{exch}^{20} term is largest at 0° and decreases upon distortion. The exchange contribution increases dramatically only when the distortion is large enough to lead to a partial overlap with the parts of the base molecule not involved in the hydrogen bond (in-plane distortion of the pyridine−HF complex, see red curve in Figure 2b). Another explanation of this small variability of the E_{exch}^{20} and $E_{exch-ind,r}^{20}$ terms is our choice of the deformation, a constant distance, variable angle approach. This could mean that the HX molecule would move along an arc of an almost constant electron density contributed by the ammonia molecule. Testing this hypothesis, we have calculated the electron density of an isolated NH_3 molecule at the MP2/aug-cc-pVTZ level. The positions of the proton of the displaced HX molecules were used as probe points. The results (included in the Supporting Information) indicate that, indeed, the angular variations of the E_{exch}^{20} and $E_{exch-ind,r}^{20}$ terms are correlated with

TABLE 2: SAPT Energy Partitioning for the $NH_3\cdots(HF)_2$ Trimer (BAA)[a]

dimer SAPT	NH_3···HF···XX	XX···HF···HF	NH_3···XX···HF	trimer SAPT	
E_{elst}^{10}	−26.950	−8.839	−3.454	E_{exch}^{10}	−0.576
E_{exch}^{10}	29.625	9.081	1.107	$E_{exch-ind}^{20}$	0.030
$E_{ind,r}^{20}$	−17.979	−4.588	−0.515	E_{ind}^{2}	−1.617
$E_{exch-ind,r}^{20}$	9.298	2.417	0.287	E_{ind}^{3}	−1.041
SCF SAPT	−6.006	−1.929	−2.576	SCF SAPT	−3.203
δHF	−6.020	−1.217	−0.059	$E_{exch-disp}^{20}$	0.093
$E_{disp,k}^{2}$	−6.685	−2.714	−0.866	E_{disp}^{3}	0.033
$E_{exch-disp}^{20}$	1.385	0.401	0.078	E_{disp}^{31}	0.006
$SAPT_{corr,r}$	−1.269	−0.208	−0.347	E_{disp}^{4}	−0.053
$SAPT_r$	−13.295	−3.355	−2.982	$SAPT_{corr}$	0.079
				SAPT	−3.125

[a] Structure optimized at the BSSE-free MP2/aug-cc-pVDZ level, energies in kcal/mol. XX denotes a molecule omitted from the trimeric structure during a particular dimer run. The first HF molecule is the one directly hydrogen-bonded to the NH_3 molecule (see Figure 3).

TABLE 3: SAPT Energy Partitioning for the $(NH_3)_2\cdots HF$ Trimer (BAB)[a]

dimer SAPT	NH_3···HF···XX	XX···HF···NH_3	NH_3···XX···NH_3	trimer SAPT	
E_{elst}^{10}	−23.807	−3.400	−5.587	E_{exch}^{10}	−0.360
E_{exch}^{10}	24.077	1.865	5.806	$E_{exch-ind}^{20}$	0.091
$E_{ind,r}^{20}$	−14.736	−0.634	−1.945	E_{ind}^{2}	−0.948
$E_{exch-ind,r}^{20}$	7.758	0.371	1.176	E_{ind}^{3}	−0.649
SCF SAPT	−6.708	−1.798	−0.550	SCF SAPT	−1.866
δHF	−4.720	−0.129	−0.556	$E_{exch-disp}^{20}$	0.089
$E_{disp,k}^{2}$	−5.772	−1.150	−2.580	E_{disp}^{3}	0.048
$E_{exch-disp}^{20}$	1.164	0.115	0.416	E_{disp}^{31}	0.003
$SAPT_{corr,r}$	−1.085	−0.463	−1.425	E_{disp}^{4}	−0.052
$SAPT_r$	−12.512	−2.390	−2.531	$SAPT_{corr}$	0.088
				SAPT	−1.778

[a] Structure optimized at the BSSE-free MP2/aug-cc-pVDZ level, energies in kcal/mol. XX denotes a molecule omitted from the trimeric structure during a particular dimer run. The first NH_3 molecule is the one directly hydrogen-bonded to the HF molecule (see Figure 4).

TABLE 4: Supermolecular Interaction Energies (BSSE-Corrected) for the BAB and BAA Trimers[a]

level of theory	NH_3···HF···HF	NH_3···HF···NH_3
MP2/aug-cc-pVDZ	−20.716	−17.849
MP2/aug-cc-pVTZ	−21.783	−18.693
MP4(SDTQ)/aug-cc-pVDZ	−20.349	−17.558
MP4(SDTQ)/aug-cc-pVTZ	−21.875	−18.863
three-body SAPT	−22.756	−19.211

[a] Structures optimized at the BSSE-free MP2/aug-cc-pVDZ level, identical to those used in the SAPT partitioning. Energies in kcal/mol. For comparison, total three-body SAPT interaction energies are added.

the electron density of the unperturbed NH_3 along the trajectory. On the other hand, the absolute values are not related to the electron density itself. The NH_3−HBr complex has the largest values of the exchange terms, but the NH_3−HCl molecule, with the longest N···H distance and thus the smallest electron density at the probe points, still has these terms larger than the NH_3−HF system. Therefore, we conclude that while the angular depencence of the E_{exch}^{20} and $E_{exch-ind,r}^{20}$ terms is governed by the density shape of the ammonia molecule, the chemical character of the hydrogen-bonded systems is revealed in the absolute values of these terms. The results support the observation that the NH_3−HBr complex has the most covalent hydrogen bond among systems investigated and that the NH_3−HCl dimer is more covalent than NH_3−HF despite having longer proton−acceptor distance.

The correlated dispersion terms (Figure 2c) are virtually constant, in agreement with the general, nondirectional character of the van der Waals forces. The total $SAPT_r$ interaction energy (Figure 2d) exhibits only small changes (ca. 1 kcal/mol) with distortions of up to 15 degrees, showing that the directionality of the hydrogen bond is much less pronounced than for the conventional covalent bond. The main reason for that is the relative angular independence of the exchange terms. According to the SAPT scheme, linear arrangement of the atoms involved in the hydrogen bond is not a result of a covalent overlap but rather of an electrostatic interaction, which prefers antiparallel orientation of the dipole moments of the interacting monomers.

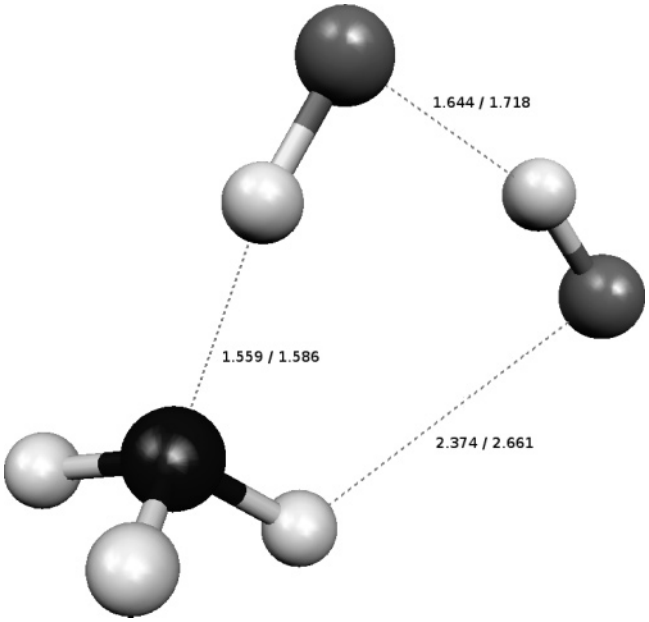

Figure 3. Structure of the cyclic $NH_3\cdots(HF)_2$ trimer optimized at the MP2/aug-cc-pVDZ level. Intermolecular distances in angstroms without/with BSSE taken into account during optimization.

3.2. The $NH_3\cdots(HF)_2$ and $(NH_3)_2\cdots HF$ Trimers. The relative importance of the three-body SAPT contributions in the $NH_3\cdots HF\cdots HF$ trimer is shown in Table 2, while the data for $NH_3\cdots HF\cdots NH_3$ is given in Table 3. Reference MP2 and MP4(SDTQ) supermolecular interaction energies are presented for comparison in Table 4. These values show that the effect of

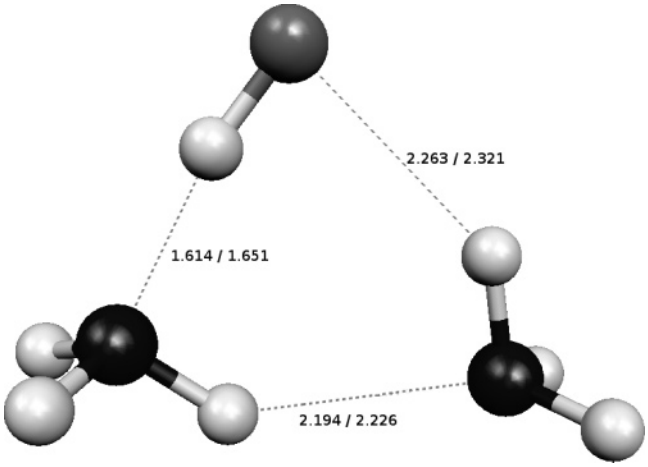

Figure 4. Structure of the cyclic $(NH_3)_2\cdots HF$ trimer optimized at the MP2/aug-cc-pVDZ level. Intermolecular distances in angstroms without/with BSSE taken into account during optimization.

the higher order perturbations seems to be small and changes sign when the basis set is increased. However, the energies are close to each other, and the best level of the theory, MP4(SDTQ)/aug-cc-pVTZ, will be compared with the SAPT results.

Both trimer structures are shown in Figures 3 and 4, respectively. The choice of the trimers was dictated by two facts. First, the component molecules are isoelectronic; second, the trimers can be labeled as belonging to the different types, that is, base−acid−acid (BAA) and base−acid−base (BAB) systems. Our disscusion of trimers begins with the BAA trimer. The total sum of partial two- and three-body SAPT interaction energies, −22.756 kcal/mol, corresponds well to the BSSE-corrected MP4/aug-cc-pVTZ supermolecular value (−21.875 kcal/mol). The three-body terms (−3.125 kcal/mol) amount to 14% of the total interaction energy. The values presented in Table 2 confirm the well-known fact[37] that most of the interaction energy nonadditivity in strongly polar systems comes from the induction terms. Stabilizing nonaddtitive exchange contributions at the uncorrelated level ($E_{exch}^{10} = -0.576$ kcal/mol) were also significant, but in total, the final three-body contribution to the SAPT interaction energy (−3.125 kcal/mol) is very close to the sum of the nonadditive induction terms ($E_{ind}^2 + E_{ind}^3 = -2.657$ kcal/mol). The three possible two-body interaction energy decompositions show that the acid−base interaction is dominating and that the acid−acid hydrogen bond was found quite weak. Interestingly, the indirect (non-hydrogen bond) ammonia−HF interaction is close in magnitude to the HF−HF energy (−2.982 and −3.355 kcal/mol, respectively), while the δHF terms differ significantly (−0.059 vs −1.217 kcal/mol). This 20-fold increase in the δHF value for the HF−HF interaction strongly suggests that it is a manifestation of the partially covalent character of the hydrogen bond. A similar pattern emerges in the case of $NH_3\cdots HF\cdots NH_3$ trimer of BAB type (Table 3 and Figure 4). Its total SAPT interaction energy, −19.211 kcal/mol, is also in good agreement with the MP4(SDTQ)/aug-cc-pVTZ supermolecular value of −18.863 kcal/mol, but the three-body terms (−1.778 kcal/mol) account for only 9% of the interaction strength. This is mostly due to the nonadditive induction terms, which are smaller than in the BAA case ($E_{ind}^2 + E_{ind}^3 = -1.597$ kcal/mol) but still dominate the three-energy contribution. The BAB trimer, in similarity to the BAA case, also has "primary" acid−base interaction of −12.5 kcal/mol and the remaining "secondary" dimeric contributions are comparable in strength to each other. Interestingly, the secondary δHF factors differ in this system not 20- but 4-fold (−0.129 kcal/mol for $HF\cdots NH_3$ and −0.556 kcal/mol for $NH_3\cdots NH_3$) and both constitute ca. 20% of their respective total secondary contributions. This is consistent with the structure of the BAB complex, which suggests that all three contacts are hydrogen bonds, contrary to the BAA case where the secondary $HF\cdots NH_3$ interaction was mostly electrostatic. Examination of the ratio between electrostatic E_{elst}^{10} and exchange E_{exch}^{10} terms shows that when they are of similar value, the δHF is also large, but when the orbital overlap (and associated E_{exch}^{10} term) is smaller, the δHF is significantly lower. This is the case for the secondary $HF\cdots NH_3$ interactions in both trimers; however, as stated above, they differ visibly in the amount of overlap. Finally, the structural effect of the BSSE is also dependent on the particular interaction strength. Figures 3 and 4 show that, in agreement with the findings of Salvador et al.,[33] the strongest interactions are least affected by the BSSE, while the secondary intermolecular distances can be severely shortened if the BSSE is not eliminated in the geometry optimization step.

4. Conclusions

The current study of the N···HX complexes revealed significant differences between hydrogen bonds of similar strength (as measured by the interaction energy). The applied SAPT partitioning showed directly the growing degree of covalency in the series of X = F, Cl, Br. The presence of an aromatic ring does not lead to significant changes of the hydrogen bond properties; the results for NH_3−HF and pyridine−HF are similar. Linear arrangement of the hydrogen bridge was a consequence of electrostatic terms. This analysis is valid for strong and middle-strength hydrogen bonds; the very strong symmetrical bridges (as FHF^-) are much more covalent. Selected trimeric cases showed that the SAPT energy partitioning is able to distinguish between hydrogen bonds and other interactions of similar strength on the basis of non-negligible covalency, revealed in the δHF term. Results presented in this study are a basis for further investigations, especially in the regime of weaker hydrogen bonds.

Acknowledgment. We would like to thank Prof. K. Szalewicz and Dr. R. Bukowski for the preprint of their publication on the three-body SAPT theory.[37] We acknowledge the generous grant of computer time at the Wrocław Center for Networking and Supercomputing, Wrocław, Poland as well as at the Academic Computer Centre CYFRONET AGH in Kraków, Poland (grants no. KBN/SGI2800/UWrocł/078/2001 and KBN/S2000/UWrocł/156/1998).

Supporting Information Available: A spreadsheet (Excel XLS format) containing the calculated energy partitioning terms for the dimers together with the electron density values of the isolated ammonia molecule measured in the location of the acidic proton. This material is available free of charge via the Internet at http://pubs.acs.org.

References and Notes

(1) Rozas, I.; Alkorta, I.; Elguero, J. *J. Phys. Chem. A* **1997**, *101*, 4236−4244.
(2) Chamberlain, A. K.; Bowie, J. U. *J. Mol. Biol.* **2002**, *322*, 497−503.
(3) Chakrabarti, P.; Chakrabarti, S. *J. Mol. Biol.* **1998**, *284*, 867−873.
(4) Chandra, A. K.; Zeegers-Huyskens, T. *J. Mol. Struct.* **2004**, *706*, 75−83.
(5) Cleland, W. W.; Kreevoy, M. M. *Science* **1994**, *264*, 1887−1890.
(6) Frey, P. A.; Whitt, S.; Tobin, J. *Science* **1994**, *264*, 1927−1930.
(7) Warshel, A.; Papazyan, A.; Kollman, P. A. *Science* **1995**, *269*, 102−104.

(8) Pan, Y.; McAllister, M. A. *J. Am. Chem. Soc.* **1997**, *119*, 7561−7566.
(9) Pan, Y.; McAllister, M. A. *J. Am. Chem. Soc.* **1998**, *120*, 166−169.
(10) Cassidy, C. S.; Lin, J.; Frey, P. A. *Biochemistry* **1997**, *36*, 4576−4584.
(11) Cleland, W. W.; Frey, P. A.; Gerlt, J. A. *J. Biol. Chem.* **1998**, *273*, 25529−25532.
(12) Riccardi, D.; Schaefer, P.; Yang, Y.; Yu, H.; Ghosh, N.; Prat-Resina, X.; Koenig, P.; Li, G.; Xu, D.; Guo, H.; Elstner, M.; Cui, Q. *J. Phys. Chem. B* **2006**, *110*, 6458−6469.
(13) Shubina, E. S.; Belkova, N. V.; Epstein, L. M. *J. Organomet. Chem.* **1997**, *536*−*537*, 17−29.
(14) Panek, J. J.; Wawrzyniak, P. K.; Latajka, Z.; Lundell, J. *Chem. Phys. Lett.* **2006**, *417*, 100−104.
(15) Hobza, P.; Havlas, Z. *Chem. Rev.* **2000**, *100*, 4253−4264.
(16) Paulson, S. L.; Barnes, A. J. *J. Mol. Struct.* **1982**, *80*, 151−158.
(17) Bulanin, M. O.; Kolomiitsova, T. D.; Kondaurov, V. A.; Melikova, S. M. *Opt. Spektrosk.* **1990**, *68*, 763.
(18) Melikova, S. M.; Rutkowski, K. S.; Rodziewicz, P.; Koll, A. *Chem. Phys. Lett.* **2002**, *352*, 301−310.
(19) Hermansson, K. *J. Phys. Chem. A* **2002**, *106*, 4695−4702.
(20) Barnes, A. J. *J. Mol. Struct.* **2004**, *704*, 3−9.
(21) Chang, B. T.; Akin-Ojo, O.; Bukowski, R.; Szalewicz, K. *J. Chem. Phys.* **2003**, *119*, 11654−11670.
(22) Valdés, H.; Sordo, J. A. *Chem. Phys. Lett.* **2003**, *371*, 386−393.
(23) Ratajczak, H. In *Electron and Proton Transfer in Chemistry and Biology*; Mueller, A., Ratajczak, H., Junge, H., Diamann, E., Eds.; Elsevier: Amsterdam, 1992; pp 293−311.
(24) Goodwin, E. J.; Howard, N. W.; Legon, A. C. *Chem. Phys. Lett.* **1986**, *131*, 319−324.
(25) Howard, N. W.; Legon, A. C. *J. Chem. Phys.* **1987**, *86*, 6722−6730.
(26) Howard, N. W.; Legon, A. C. *J. Chem. Phys.* **1988**, *88*, 4694−4701.
(27) Novick, S. E.; Leopold, K. R.; Klemperer, W. In *Atomic and Molecular Clusters*; Bernstein, E. R., Ed.; Elsevier: Amsterdam, 1990; pp 359−391.
(28) Biczysko, M.; Latajka, Z. *Chem. Phys. Lett.* **1999**, *313*, 366−373.
(29) Biczysko, M.; Latajka, Z. *J. Phys. Chem. A* **2002**, *106*, 3197−3201.
(30) Woon, D. E.; Dunning, T. H., Jr. *J. Chem. Phys.* **1993**, *98*, 1358−1371.
(31) Kendall, R. A.; Dunning, T. H., Jr.; Harrison, R. J. *J. Chem. Phys.* **1992**, *96*, 6796−6806.
(32) Frisch, M. J.; Trucks, G. W.; Schlegel, H. B.; Scuseria, G. E.; Robb, M. A.; Cheeseman, J. R.; Montgomery, J. A., Jr.; Vreven, T.; Kudin, K. N.; Burant, J. C.; Millam, J. M.; Iyengar, S. S.; Tomasi, J.; Barone, V.; Mennucci, B.; Cossi, M.; Scalmani, G.; Rega, N.; Petersson, G. A.; Nakatsuji, H.; Hada, M.; Ehara, M.; Toyota, K.; Fukuda, R.; Hasegawa, J.; Ishida, M.; Nakajima, T.; Honda, Y.; Kitao, O.; Nakai, H.; Klene, M.; Li, X.; Knox, J. E.; Hratchian, H. P.; Cross, J. B.; Bakken, V.; Adamo, C.; Jaramillo, J.; Gomperts, R.; Stratmann, R. E.; Yazyev, O.; Austin, A. J.; Cammi, R.; Pomelli, C.; Ochterski, J. W.; Ayala, P. Y.; Morokuma, K.; Voth, G. A.; Salvador, P.; Dannenberg, J. J.; Zakrzewski, V. G.; Dapprich, S.; Daniels, A. D.; Strain, M. C.; Farkas, O.; Malick, D. K.; Rabuck, A. D.; Raghavachari, K.; Foresman, J. B.; Ortiz, J. V.; Cui, Q.; Baboul, A. G.; Clifford, S.; Cioslowski, J.; Stefanov, B. B.; Liu, G.; Liashenko, A.; Piskorz, P.; Komaromi, I.; Martin, R. L.; Fox, D. J.; Keith, T.; Al-Laham, M. A.; Peng, C. Y.; Nanayakkara, A.; Challacombe, M.; Gill, P. M. W.; Johnson, B.; Chen, W.; Wong, M. W.; Gonzalez, C.; Pople, J. A. *Gaussian 03*, Revision C.02; Gaussian, Inc.: Wallingford, CT, 2004.
(33) Salvador, P.; Paizs, B.; Duran, M.; Suhai, S. *J. Comput. Chem.* **2001**, *22*, 765−786.
(34) Jeziorski, B.; Moszyński, R.; Szalewicz, K. *Chem. Rev.* **1994**, *94*, 1887−1930.
(35) Bukowski, R.; Cencek, W.; Jankowski, P.; Jeziorski, B.; Jeziorska, M.; Kucharski, S. A.; Misquitta, A. J.; Moszyński, R.; Patkowski, K.; Rybak, S.; Szalewicz, K.; Williams, H. L.; Wormer, P. E. S. *SAPT2002: An Ab Initio Program for Many-Body Symmetry-Adapted Perturbation Theory Calculations of Intermolecular Interaction Energies. Sequential and Parallel Versions*; University of Delaware and University of Warsaw, 2002; see http://www.physics.udel.edu/∼szalewic/SAPT/SAPT.html.
(36) Schmidt, M. W.; Baldridge, K. K.; Boatz, J. A.; Elbert, S. T.; Gordon, M. S.; Jensen, J. H.; Koseki, S.; Matsunaga, N.; Nguyen, K. A.; Su, S. J.; Windus, T. L.; Dupuis, M.; Montgomery, J. A. *J. Comput. Chem.* **1993**, *14*, 1347−1363.
(37) Szalewicz, K.; Bukowski, R.; Jeziorski, B. In *Theory and Applications of Computational Chemistry;* Dykstra, C., Frenking, G., Kim, K., Scuseria, G., Eds.; Elsevier: Boston, MA, 2005; Chapter 33.
(38) Portmann, S.; Lüthi, H. P. *Chimia* **2000**, *54*, 766−770.
(39) Grabowski, S. J.; Sokalski, W. A. *J. Phys. Org. Chem.* **2005**, *18*, 779−784.
(40) Silvi, B.; Savin, A. *Nature* **1994**, *371*, 683−686.
(41) Poater, J.; Duran, M.; Solà, M.; Silvi, B. *Chem. Rev.* **2005**, *105*, 3911−3947.
(42) Fuster, F.; Silvi, B. *Theor. Chem. Acc.* **2000**, *104*, 13−21.
(43) *NIST Computational Chemistry Comparison and Benchmark Database*; NIST Standard Reference Database Number 101 Release Aug 12, 2005; Johnson, R. D., III, Ed. http://srdata.nist.gov/cccbdb.